submitted to GRL

The role of coupled feedbacks in the decadal variability of the SH eddy-driven jet

Dongxia Yang[1], Julie M. Arblaster[1,2], Gerald A. Meehl[2], Matthew H. England[3]

1. ARC Centre of Excellence for Climate Extremes, Monash University, Australia
2. National Center for Atmospheric Research, Boulder, CO, USA
3. ARC Centre of Excellence for Climate Extremes, Climate Change Research Centre, University of New South Wales, Sydney, Australia

January 15, 2021

*Corresponding author: Dongxia Yang
School of Earth, Atmosphere and Environment,
Monash University, Clayton Campus,
VIC 3800.
E-mail: dongxia.yang@monash.edu

Key points:

--Coupled and uncoupled pacemaker experiments are conducted to investigate the influence of tropical Pacific decadal variability on Southern Hemisphere eddy-driven jet

--South Pacific jet responds to the tropical Pacific sea surface temperature (SST) variability via direct atmospheric processes

--Air-sea coupling is notably important to reproduce the observed poleward migration of South Atlantic-Indian jet

Abstract:

Recent work has suggested that tropical Pacific decadal variability and external forcings have had a comparable influence on the observed changes in the Southern Hemisphere (SH) summertime eddy-driven jet over the satellite era. Here we contrast the zonally asymmetric response of the SH eddy-driven jet to tropical Pacific decadal variability using ensembles of the Community Earth System Model version 1 (CESM1) in a pacemaker framework, where sea surface temperatures (SSTA) in the tropical Pacific are nudged to observations. In both coupled and uncoupled experiments, the observed South Pacific jet intensification is found in all seasons, indicating the tropical Pacific SST cooling anomaly impacts the South Pacific jet mainly via direct atmospheric processes. By contrast, only the coupled pacemaker reproduces the South Atlantic-Indian jet poleward shift in the summertime, suggesting that the air-sea coupling is essential in driving the teleconnections between tropical Pacific SSTA and South Atlantic-Indian jet variations.

Plain language summary:

There is a zonally asymmetric response of the Southern Hemisphere eddy-driven jet to tropical Pacific decadal variability, with a poleward migration observed in the South Atlantic-Indian basin and an intensification for the South Pacific basin. Using ensembles of the Community Earth System Model version 1 (CESM1) tropical Pacific pacemaker experiments in both coupled and uncoupled frameworks, we found South Pacific jet responds to the tropical Pacific sea surface temperature (SST) variability via direct atmospheric processes. By contrast, the air-sea coupling is notably important in South Atlantic-Indian basin to enable the Pacific–South American (PSA) Rossby wave pattern.

1. Introduction:

Observational and model studies have shown that the Southern Hemisphere (SH) summertime (December-January-February, DJF) eddy-driven jet experienced a poleward shift during the last four decades, along with a positive trend in the Southern Annular Mode (SAM). Along with the dominant impact of SH stratospheric ozone depletion on these trends, as discussed in previous research (Banerjee et al., 2020; Lee & Feldstein, 2013; Polvani et al., 2011), the role of tropical sea surface temperature (SST) variations has also recently been emphasized (Deser & Phillips, 2009; Schneider et al., 2015; Yang et al., 2020). In particular, Yang et al. (2020) examined the separate influence of internally generated decadal variability from tropical Pacific, Indian and Atlantic basin SSTs on the position and strength of the SH eddy-driven jet. Using the CESM1 pacemaker experiments, they found the decadal changes of tropical Pacific SSTs and external forcing played comparable roles in the poleward jet shift between the 1979-1998 and 1999-2013 periods.

In addition, Yang et al. (2020) pointed out that in both the observations and response to tropical Pacific SSTs, the summertime eddy-driven jet experiences an intensification in the South Pacific with a deepened Amundsen Sea Low (ASL), unlike the poleward movement in the South Atlantic and South Indian basins. These zonal asymmetric jet variations are also described by Waugh et al. (2020) for the DJFMAM seasons, i.e. the South Pacific jet underwent a strengthening in contrast to the latitudinal position change in the South Atlantic-Indian basins. The tropical Pacific - South Pacific teleconnection has been widely discussed in previous studies, for example, Irving and Simmonds (2016) suggested that the interannual to interdecadal tropical SST trends over 1979-2014 can influence the SH high latitudes and regional Antarctic climate via an anomalous Pacific–South American (PSA) Rossby wave pattern. Meehl et al. (2016) linked the negative phase of the Interdecadal Pacific Oscillation (IPO) during 2000-2014 to the Ross Sea and Amundsen Sea sea ice changes via a positive phase of the SAM combined with a deepened Amundsen Sea Low (ASL).

By contrast, the tropical Pacific remote impact on the South Atlantic/Indian atmospheric circulation has been less studied and previous work mainly attributes this remote connection to the downstream effect of the PSA. For instance, Rodrigues et al. (2015) found in response to La Niña events and its induced positive PSA pattern, a northeast-southwest South Atlantic SST dipole develops with a warming (cooling) anomaly around 40°S (20°S); Similar results are attained at the interdecadal time scales, where Lopez et al. (2016) found South Atlantic SST and sea surface height (SSH) dipole variability is remotely modulated by the IPO via PSA wave trains.

However, both a strength and a weakness of the coupled pacemaker framework in Yang et al. (2020) is that this allows coupled feedbacks in response to the region of prescribed SSTs. These inter-basin interactions, particularly between the tropical oceans (Cai et al., 2019), make it difficult to separate the direct atmospheric influence of the tropical Pacific SSTs. Hence an outstanding question arises: What is the role of air-sea coupling in the teleconnection between tropical Pacific SSTs and the SH mid-latitude circulation?

Yang et al. (2020) argue that the South Pacific jet intensification was primarily induced by internal fluctuations from tropical Pacific SST. However, other studies also suggest the South Pacific Convergence Zone (SPCZ) could potentially modulate the South Pacific mid-to-high latitude circulation response to tropical Pacific SSTA (Clem et al., 2019; Meehl et al., 2016; Meehl et al., 2019). For example, using atmospheric heating experiments, Meehl et al. (2016)

found that for the DJF season, the eastern Pacific cooling would induce a deepened Amundsen Sea Low (ASL) while the SPCZ warming would lead to a shallowed ASL instead, with the latter more consistent with observed changes in that season. Consistent results are obtained by Clem et al. (2019) for the DJFMAM season where a 2°C SSTA was prescribed over the SPCZ using the CAM5 model. However, both studies used idealised experiments and the separate influence of tropical eastern Pacific and SPCZ SST anomalies on the SH circulation using realistic SSTs over recent decades has yet to be explored.

Variations in the mid-latitude jet and the associated SAM and ASL patterns have a large impact on the Southern Ocean circulation and Antarctic sea ice change. Lefebvre et al. (2004) suggested that the response of circumpolar Southern Ocean to positive SAM includes an annular component with a northward surface Ekman drift and a non-annular component characterised by a sea ice increase in the Ross Sea and a decrease in the Weddell Sea. Purich et al. (2016) found that disparities between the CMIP5 ensemble-averaged Antarctic sea ice decline and the observed expansion over 1979-2013 could be attributed in part to the weakly simulated jet intensity in the CMIP5 models.

There remain questions regarding the mechanism driving the zonal asymmetric South Pacific jet response to the tropical Pacific SST and the importance of coupled feedbacks to the jet response in general. Therefore, two main questions would be addressed in this paper:

1. What is the role of air-sea coupling in the tropical Pacific SST and SH eddy-driven jet teleconnections?

2. What are the relative influences of tropical eastern Pacific and SPCZ SSTA on ASL and eddy-driven jet variations?

The structure of this paper is organized as follows. The experimental design is specified in Section 2. The main results are presented in Section 3. A brief summary and discussion are outlined in Section 4.

2. Experiment Design:

Following Yang et al. (2020), here we used the fully coupled CESM1 40-member Large Ensemble mean (LENS) to estimate the impact of external forcing; and the 10-member Pacific pacemaker ensemble mean (PACE) minus LENS to infer the influence of internally-driven tropical Pacific SST (See Table 1).

All LENS ensemble members are constrained to the same radiative forcing scenario (Taylor et al. 2012), with historical forcing during 1920-2005 and a high emission forcing scenario of the Representative Concentration Pathway (RCP) 8.5 (Moss et al., 2010) from 2006 to 2080. The initial conditions of each LENS ensemble member are perturbated with a small atmospheric temperature disturbance, which then evolves into a diverse member spread and produces 40 different realizations of internal climate variability. The LENS 40-member ensemble mean averages out this random internal variability and reflects the influence of external radiative forcings on the climate system.

The Pacific pacemaker uses the same model and anthropogenic radiative forcing as LENS but the SST anomalies (SSTA) in the tropical eastern Pacific (15°S-15°N, 175°E to the American coast, with two buffer belts along 15°S-20°S and 15°N-20°N as well as a another buffer zone at 175°E-180°) are restored to the observed anomalies from NOAA Extended Reconstruction Sea Surface Temperature, version 3b (Smith et al., 2008). Therefore, the PACE ensemble mean contains both the radiatively forced and internal variability generated by the tropical Pacific SSTs, and PACE minus LENS removes external forcing and estimates the response of the global climate system to the observed time-varying Pacific SSTs.

However, in the coupled Pacific pacemaker, where the SSTAs over the eastern Pacific region are nudged to observations and the rest of the model is free to evolve (Table 1 and Fig. 1c), the tropical Pacific SSTA forcing promotes an SST response in other regions, which can then force a secondary teleconnection and influence the mid-latitude jet. To remove the compounding effects of Pacific coupling to other ocean basins, an atmosphere-only simulation "Pacific Ocean-Global Atmosphere (POGA)" is designed to compare with the Pacific pacemaker. This POGA experiment is intended to match the tropical Pacific pacemaker in many ways. It uses the same atmospheric model as in the pacemaker (CAM5) and is subjected to an identical external forcing scenario. The SST forcing is prescribed using the monthly Pacific pacemaker SSTs in the tropical eastern Pacific region, and the time-varying CESM LENS 40-member ensemble mean monthly SSTs is imposed elsewhere. In this way, the POGA 10-member ensemble mean with external forcing removed (ie., POGA minus LENS) isolates the direct atmospheric influence of internally-driven tropical Pacific SST on SH atmospheric circulation from any secondary teleconnections.

We make one alteration to the nudging region in the POGA experiment by extending the western boundary of the nudged SST region from 175°W (in pacemaker, boxes on Fig. 1c) to 165°E (in POGA, Fig. 1d). This better mimics the coupled pacemaker experiment which naturally extends the anomalies related to these oscillations to the west of its nudged region and allows a comprehensive impact of the main tropical Pacific variability like the IPO and El Niño–Southern Oscillation (ENSO) patterns.

Another uncoupled experiment (hereafter named ext-SPCZ), with Pacific pacemaker SSTs applied over 35°S-20°N, 165°E-the American coast (Fig. 1e), is also conducted to further investigate the relative roles of observed tropical eastern Pacific and SPCZ SSTAs. Since POGA and ext-SPCZ are identical except for the expanded nudged region, comparisons between ext-SPCZ and POGA isolates the impact of the SPCZ SSTA on the atmospheric teleconnection patterns in the SH mid-to-high latitudes.

3. Results:

3.1. Tropical Pacific pacemaker and POGA comparison

Based on the IPO phase transition (positive to negative) around 1999, and to follow Yang et al. (2020), here we separated the satellite era into two periods 1980-1998 (P1) and 1999-2013 (P2). Fig.1 shows the decadal difference (P2 average minus P1 average) of SST for observations and model simulations. In observations (Fig. 1a) and in all simulations by design, the nudged region of the Pacific basin displays a negative phase of the IPO pattern, with large cooling anomalies over the eastern and central Pacific. Outside of the nudged region, it is clear that the coupled pacemaker combines 1) the atmospheric influence caused by eastern Pacific SST and 2) the secondary impact of evolved SST variations in other basins. Specifically, in PACE minus LENS (Fig. 1c), the negative convective heating anomaly over the eastern Pacific cooling promotes a warming over the South Pacific Convective Zone (SPCZ) and the South Atlantic Convective Zone (SACZ) regions. This is consistent with Clem et al. (2019) who argued that cooling in the eastern Pacific can induce a warming anomaly in the SPCZ region as part of the negative IPO pattern. The negative IPO induced SACZ warming anomaly in Fig. 1c is also consistent with (Lopez et al., 2016) in terms of the decadal teleconnections between the negative IPO and South Atlantic SST changes. By contrast, POGA isolates the direct atmospheric impact of tropical Pacific SSTAs alone.

As for the summertime eddy-driven jet variations, the South Pacific jet displays an intensification instead of a latitudinal movement in both observation and the coupled pacemaker (Fig. 2a and 2c), which is distinct from the poleward shift in the Atlantic and Indian basins. The POGA experiment also successfully reproduces the jet strengthening in the South Pacific basin (Fig. 2d) but fails to capture the poleward movement of the jet over the South Atlantic-Indian basins. Differences between the uncoupled POGA and coupled pacemaker (Fig. 2c and Fig. 2d, with external forcing removed) implies that the influence of tropical Pacific SST on South Pacific jet intensification is mainly via the atmospheric processes. It is also clear that for the teleconnections between the tropical Pacific SST and South Atlantic-Indian jet variations, air-sea coupling is critical since the observed poleward shift of the jet in those basins is only reproduced in the coupled pacemaker experiment.

Consistent results are found in the sea level pressure field. A positive SAM phase is observed and simulated in the pacemaker but not in the POGA for the South Atlantic-Indian basin, highlighting that coupling is important to establish the teleconnections between the tropical Pacific and the South Atlantic-Indian basin. In the South Pacific basin, the deepened ASL and 30°S high-pressure anomaly is captured in both pacemaker and POGA ensemble mean.

This tropical-extratropical teleconnection within the Pacific basin is also detected in the other three seasons. The most significant South Pacific jet shift is observed in the MAM season (Schneider et al., 2015). In accordance with the strengthened South Pacific jet (Fig. S1a) in austral autumn, a deepened ASL (Fig. S1f) is observed and also largely reproduced by the POGA but not by the pacemaker ensemble mean. In austral winter-spring seasons (June-July-August, September-October-November, JJA in Fig. S2 and SON in Fig. S3), the observed South Pacific eddy-driven jet exhibits an equatorward shift (Waugh et al., 2020), where both POGA and pacemaker ensemble mean captured this pattern. These further verify that the South Pacific westerly variation in all seasons is mainly induced by the direct atmospheric teleconnections from tropical Pacific SSTA. In the non-summer seasons, the South Atlantic-Indian jet exhibits less uniform changes in intensity and position compared to the DJF season, and neither pacemaker nor POGA can fully reproduce the South Atlantic-Indian jet variation, indicating there are other factors beyond tropical Pacific SSTA that drive the South Atlantic-Indian jet changes outside of the summertime.

3.2. POGA and ext-SPCZ comparison

Differences between the POGA and pacemaker in the South Atlantic-Indian jet simulations indicate that tropical Pacific SSTs could influence the SH jet by modifying SSTs in other basins first. Based on Fig. 1c, the eastern Pacific SST cooling develops a warming belt in the SH subtropical area in each basin, including the SPCZ, SACZ and the South Indian convergence zone (SICZ). Previous studies (Meehl et al. 2016; Clem et al. 2019) suggest that SPCZ warming shallows the ASL in the DJF-MAM seasons, playing an opposite role to eastern Pacific SST cooling.

Accordingly, another experiment is conducted to further investigate the relative roles of eastern Pacific SST cooling and its provoked SPCZ warming. Comparison between POGA (Fig. 2d/i) and ext-SPCZ (Fig. 2e/j) shows a subtle difference in the South Pacific jet variation, namely the jet intensified centre slightly shifts to the east and the low-pressure centre moves from the Ross Sea to the Amundsen Sea, making it more consistent with the observations and pacemaker. The ext-SPCZ captures a slight poleward shift in the jet in the South Indian basin, which is in better agreement with the pacemaker results than POGA, suggesting that SPCZ warming may be important for the teleconnections between tropical SST and South Indian jet variations. However, in the South Atlantic basin, neither POGA nor ext-SPCZ reproduces the southward movement in the jet as in observations and in the pacemaker. Subtracting Fig. 2d from Fig. 2e isolates the SPCZ impact, which reveals the eastern Pacific cooling is a main driver of the DJF South Pacific jet strengthening and that contributions from the SPCZ warming is relatively small. Similar relations can be found in the other three seasons (Fig. S1 - Fig. S3).

4. Mechanism: Poleward propagation of Rossby waves

Early studies imply that tropical Pacific SSTs can impact the extratropical circulation via the poleward propagation of PSA stationary Rossby waves (Hoskins & Karoly, 1981), and recent work further suggests the SPCZ SSTA as an additional hotspot for PSA wave sources (Clem et al., 2019; Lopez et al., 2016). Here we examine this teleconnection at the decadal timescales in the uncoupled runs and compare with the coupled pacemaker to identify the role of air-sea coupling.

For the observed SST decadal difference, there is a cooling of the central tropical Pacific SST (Fig. S4a, same as Fig. 1a) as noted earlier, which leads to reduced precipitation with descending air (Fig. S4b, the largest negative values occur on and just south of the Equator), and less outgoing longwave radiation over that same area (Fig. S4c). The positive OLR anomaly coincides with an upper troposphere horizontal convergence in the central Pacific (negative geopotential height anomaly at 200 hPa, Fig. 3a/ Fig. S4d). Mirroring the tropical Pacific cooling, there is also significant warming over the SPCZ near 30°S. This region shows opposite tendencies compared to the tropical central Pacific, with enhanced rainfall, negative OLR and a positive 200 hPa geopotential height anomaly. These two centres (central Pacific cooling and SPCZ warming), act as Rossby wave sources for the extratropics (Clem et al., 2019). As a consequence, the SH circulation shows positive sea level pressure anomalies over mid-latitudes and negative sea level pressure anomalies over high-latitudes, resulting in a positive SAM phase (Fig. 3a and Fig. 2f).

The Pacific pacemaker (external forcing removed) captures most features in the observations, with a cooling SSTA, associated decreased rainfall, positive OLR and upper-level convergence in the central Pacific, as well as a warming SSTA and increased rainfall over the SPCZ (Fig. S 4e-h). The PSA pattern produced by the Pacific pacemaker (external forcing removed) is much clearer and more zonal asymmetric compared to observations, with distinguished low-high geopotential height wave trains propagating from the tropical Pacific to the subtropical South Atlantic via South America cape (Fig. 3b). In contrast, in POGA (external forcing removed), the PSA seems to fade away after turning around the south of the South America (Fig. 3c), though in the South Pacific basin, the mid-latitude positive pressure anomaly and deepened ASL is well reproduced. Comparisons between POGA and pacemaker thus highlight the importance of coupling in the PSA wave pattern and in maintaining the tropical Pacific- South Atlantic-Indian teleconnections.

The combined impact of tropical Pacific cooling and SPCZ warming (Fig. 3d) exhibits a similar Rossy wave pattern to POGA in the South Pacific basin, although the deepened low shifts slightly east from the Ross Sea (in POGA) to the Amundsen Sea (in ext-SPCZ), which is in closer agreement with the pacemaker and consistent with the jet (Fig. 2e) and SLP (Fig. 2i) variations. In the South Indian basin, the positive SAM-like pattern is better captured in ext-SPCZ, indicating SPCZ warming could be bridging the teleconnections between tropical SSTA and South Indian jet variations. This additive influence of tropical Pacific cooling and SPCZ warming on the ASL seems to be contrary to Clem et al. (2019) indicating during the DJFMAM season, where the SPCZ warming plays an opposite role to the eastern Pacific cooling by shallowing the ASL. However, in our work, we find that the SH summertime ASL longitudinal location is improved with SPCZ but its intensity does not vary much with/without SPCZ warming. Another potential source of this difference is that Clem et al. (2019) imposes a fixed +2°C SSTA over the SPCZ region, instead of the observed SSTA used in this study. If the combined impact of SPCZ warming and tropical Pacific cooling is not linearly additive, this could cause a significant difference from the observations.

5. Summary and Discussions

Recent work has suggested that the IPO has made a major contribution to the SH summertime eddy-driven jet variations over the satellite era, including the strengthening of the South Pacific jet and poleward shift of the South Atlantic-Indian jet. One of the remaining questions, however, was whether tropical Pacific SSTs influence the SH jet via direct atmospheric teleconnections or by changing SSTs in other basins. In this study, we tried to address this question by using ensembles of CESM1 tropical Pacific pacemaker experiments in both coupled and uncoupled frameworks. In both frameworks, the tropical Pacific sea surface temperatures (SSTs) are nudged to identical time-varying observed anomalies. In the coupled experiments, SSTs in other basins can respond to the tropical Pacific through inter-basin interactions, whereas in the uncoupled experiments (POGA) the SSTs are prescribed.

We found that in all seasons, the uncoupled POGA could capture the observed eddy-driven jet variation in the South Pacific basin, including the equatorward shift in the JJA-SON seasons and strengthening during DJF-MAM. This indicates that the South Pacific eddy-driven jet responds to tropical SST mainly via atmospheric pathways. Comparisons between pacemaker and POGA show that the air-sea coupling is notably more important in forcing the South Atlantic-Indian basin to enable the PSA Rossby wave propagation. A further uncoupled experiment ext-SPCZ was conducted to investigate the relative roles of tropical Pacific and SPCZ convective centres for the above teleconnections. Comparisons between POGA and ext-SPCZ stressed the importance of the SPCZ in bridging the PSA Rossby wave pattern, generating a more realistic ASL position and South Indian jet variations.

Yang et al. (2020) pointed out that in observation and in the coupled pacemaker, a significant air temperature warming anomaly is found throughout the troposphere at 45°S in response to the anomalously cool tropical Pacific SSTs, which then leads to an enhanced meridional temperature gradient, increased near-surface baroclinity, more transient eddy generation in high latitudes and a poleward shifted eddy-driven jet. We also examined the air temperature distribution in the uncoupled experiments (Fig. S6), but instead of zonal mean metrics in Yang et al. (2020), here we examined the South Pacific and Atlantic-Indian basins separately. In the South Pacific basin, both POGA and ext-SPCZ could reproduce the warming anomaly throughout the troposphere as in the pacemaker, though with a smaller magnitude (Fig. S6c-S6d). However, over the South Atlantic-Indian region, different from the large warming belt in the pacemaker, POGA barely generates any warming anomaly in the SH mid-latitudes (Fig. S6g), which results in less tropic-to-pole temperature contrast and less near-surface baroclinity generation. This could potentially be related to the disparities in the simulation of

Atlantic-Indian jet latitudinal position between pacemaker and POGA. The South Atlantic-Indian temperature contrast and jet movements in ext-SPCZ lie between POGA and the pacemaker, ie., the warming belt in ext-SPCZ (Fig. S6h) is larger than POGA but much weaker compared to the pacemaker, resulting in a moderate meridional temperature gradient and poleward shift of the Indian jet (Fig. 4j).

In conclusion, our model results indicate that tropical Pacific SST influences the South Pacific jet decadal variation mainly via direct atmospheric pathway, which is consistent with Waugh et al. (2020). In contrast, we found for the South Atlantic-Indian basins, the air-sea coupling is more important, where tropical Pacific SST prompted SPCZ and SACZ warming could play a role in the PSA pattern propagation.

Our findings could provide useful references for future air-sea-ice coupling studies. For instance, the zonal asymmetric wind forcing instead of zonal-mean SAM-like winds for ocean/sea-ice model studies, which could potentially lead to more accurate sea ice longitudinal prediction over the Amundsen Sea and Ross Sea region. In addition, the uncoupled POGA and coupled pacemaker simulations enable an apple-to-apple comparison to identify the tropical Pacific SST influence on the global SST and atmospheric circulation. Understanding the role of tropical internal variability on the SH eddy-driven jet is critical to understanding past and future changes in the Southern Ocean circulation and Antarctic sea-ice and ice sheets.

Acknowledgements

This work was supported by 1) the Australian Research Council Centre of Excellence for Climate Extremes (grant CE170100023); 2) the Regional and Global Model Analysis (RGMA) component of the Earth and Environmental System Modeling Program of the U.S. Department of Energy's Office of Biological & Environmental Research (BER) Cooperative Agreement # DE-FC02-97ER62402; 3) the National Center for Atmospheric Research, which is a major facility sponsored by the National Science Foundation under Cooperative Agreement No. 1852977. Most figures were created using NCAR Command Language (NCL) version 6.5.0. Computing resources (doi:10.5065/D6RX99HX) were provided by the Climate Simulation Laboratory at NCAR's Computational and Information Systems Laboratory. We also thank Adam Phillips (from NCAR), Shayne McGregor (from Monash University), and Harry Hendon (from the Australian Bureau of Meteorology) for helpful discussions.

6. Reference

Banerjee, A., Fyfe, J. C., Polvani, L. M., Waugh, D., and Chang, K.-L. (2020), A pause in Southern Hemisphere circulation trends due to the Montreal Protocol, *Nature*, *579*(7800), 544-548.

Cai, W., Wu, L., Lengaigne, M., Li, T., McGregor, S., Kug, J.-S., et al. (2019), Pantropical climate interactions, *Science*, *363*(6430), eaav4236.

Clem, K. R., Lintner, B. R., Broccoli, A. J., and Miller, J. R. (2019), Role of the South Pacific Convergence Zone in West Antarctic Decadal Climate Variability, *Geophys. Res. Lett.*

Deser, C., and Phillips, A. S. (2009), Atmospheric Circulation Trends, 1950–2000: The Relative Roles of Sea Surface Temperature Forcing and Direct Atmospheric Radiative Forcing, *Journal of Climate*, *22*(2), 396-413.

Irving, D., and Simmonds, I. (2016), A New Method for Identifying the Pacific–South American Pattern and Its Influence on Regional Climate Variability, *Journal of Climate*, *29*(17), 6109-6125.

Lee, S., and Feldstein, S. B. (2013), Detecting ozone-and greenhouse gas–driven wind trends with observational data, *Science*, *339*(6119), 563-567.

Lefebvre, W., Goosse, H., Timmermann, R., and Fichefet, T. (2004), Influence of the Southern Annular Mode on the sea ice–ocean system, *Journal of Geophysical Research: Oceans*, *109*(C9).

Lopez, H., Dong, S., Lee, S. K., and Campos, E. (2016), Remote influence of Interdecadal Pacific Oscillation on the South Atlantic meridional overturning circulation variability, *Geophys. Res. Lett.*, *43*(15), 8250-8258.

Moss, R. H., Edmonds, J. A., Hibbard, K. A., Manning, M. R., Rose, S. K., Van Vuuren, D. P., et al. (2010), The next generation of scenarios for climate change research and assessment, *Nature*, *463*(7282), 747.

Polvani, L. M., Waugh, D. W., Correa, G. J., and Son, S.-W. (2011), Stratospheric ozone depletion: The main driver of twentieth-century atmospheric circulation changes in the Southern Hemisphere, *Journal of Climate*, *24*(3), 795-812.

Purich, A., Cai, W., England, M. H., and Cowan, T. (2016), Evidence for link between modelled trends in Antarctic sea ice and underestimated westerly wind changes, *Nature Communications*, *7*, 10409.

Rodrigues, R. R., Campos, E. J., and Haarsma, R. (2015), The impact of ENSO on the South Atlantic subtropical dipole mode, *Journal of Climate*, *28*(7), 2691-2705.

Schneider, D. P., Deser, C., and Fan, T. (2015), Comparing the Impacts of Tropical SST Variability and Polar Stratospheric Ozone Loss on the Southern Ocean Westerly Winds, *Journal of Climate*, *28*(23), 9350-9372.

Smith, T. M., Reynolds, R. W., Peterson, T. C., and Lawrimore, J. (2008), Improvements to NOAA's historical merged land–ocean surface temperature analysis (1880–2006), *Journal of Climate*, *21*(10), 2283-2296.

Waugh, D. W., Banerjee, A., Fyfe, J. C., and Polvani, L. M. (2020), Contrasting recent trends in Southern Hemisphere Westerlies across different ocean basins, *Geophys. Res. Lett.*, e2020GL088890.

Yang, D., Arblaster, J. M., Meehl, G. A., England, M. H., Lim, E.-P., Bates, S., and Rosenbloom, N. (2020), Role of tropical variability in driving decadal shifts in the Southern Hemisphere summertime eddy-driven jet, *Journal of Climate*, *33*(13), 5445-5463.

Table 1 Summary of the CESM and CAM5 experiments used in this paper.

Experiments	External forcing	Nudged/Prescribed SSTs	Members
Large Ensemble (LENS)	Historical for 1920-2005, RCP8.5 for 2006-2013	—	40
Pacific Pacemaker (PACE)	Same as LENS, except with SPARC ozone forcing	*Fully-restored SSTA for 15°S-15°N, buffer belts for 15-20°S & 15-20°N, 175°W to the American coast.*	10
POGA	Same as Pacemaker	*Pacific pacemaker SST for* ***15°S-15°N,*** *165E° to the American coast; 40-member-mean LENS outside of eastern Pacific, buffer belts for 15-20°S & 15-20°N, 150-165°E.*	10
ext-SPCZ	Same as Pacemaker	*Pacific pacemaker SST for* ***35°S-15°N****, 165E° to the American coast; 40-member-mean LENS outside of eastern Pacific, buffer belts for 35-40°S & 15-20°N, 150-165°E.*	10

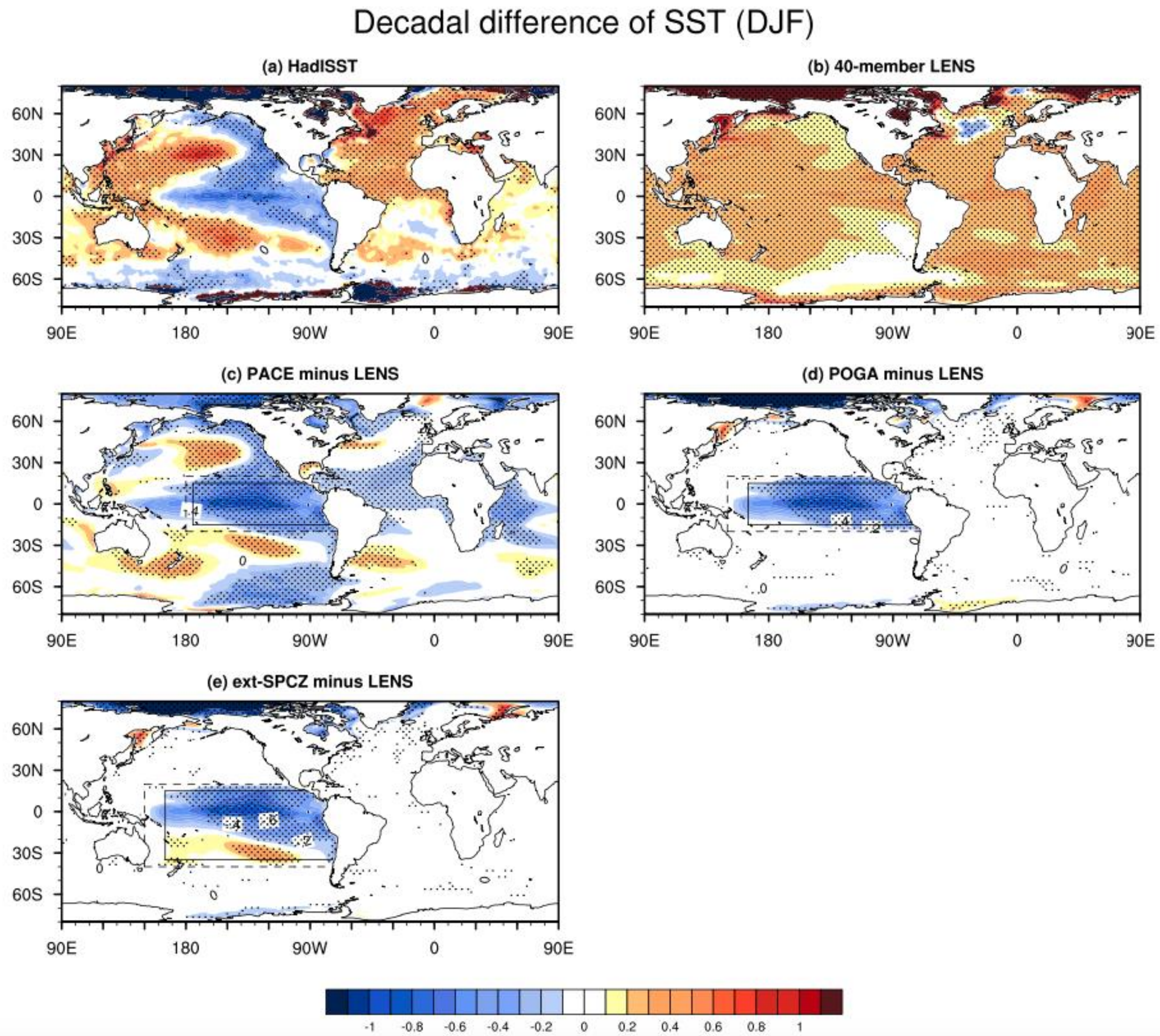

Figure 1. The decadal difference between averaged P2 (1999-2013) and P1 (1979-1998) for sea surface temperature (K). (a) HadISST; (b) CESM Large Ensemble mean (LENS), indicative of external forcing; (c) Pacific pacemaker ensemble-mean (PACE) minus LENS; (d) POGA ensemble-mean minus LENS; (e) ext-SPCZ ensemble-mean minus LENS. Stippling indicates differences are significant at the 90% for (a) and 95% level for all other panels, based on a t-test.

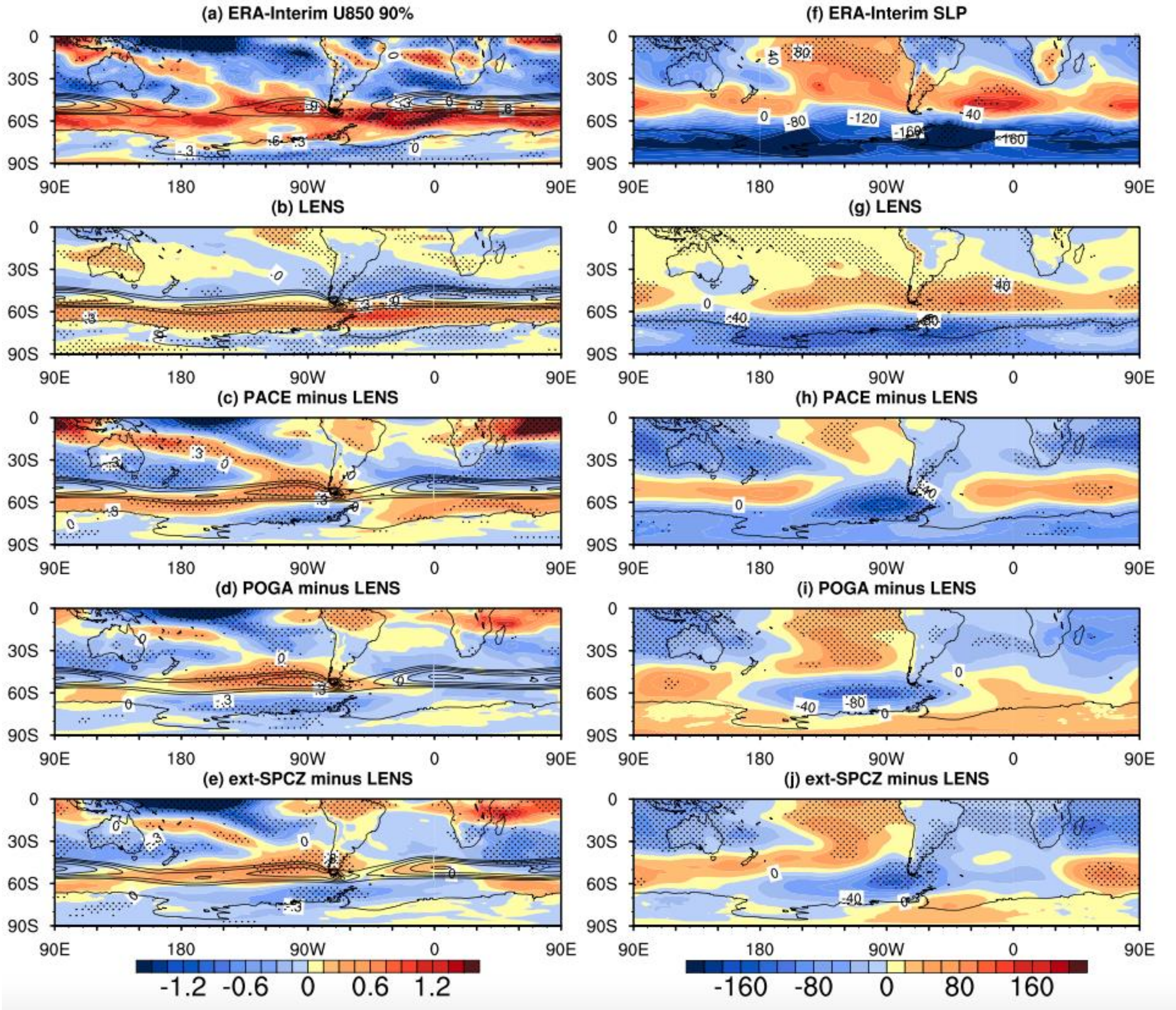

Figure 2. The decadal difference between averaged P2 (1999-2013) and P1 (1979-1998) for 850 hPa zonal wind (left, unit: m/s) and SLP (right, unit: Pa) in DJF season. (a/f) ERA-Interim; (b/g) LENS; (c/h) PACE minus LENS; (d/i) POGA minus LENS; (e/j) ext-SPCZ minus LENS. Stippling indicates differences are significant at the 90% level for (a) and 95% level for all other panels, based on a t-test.

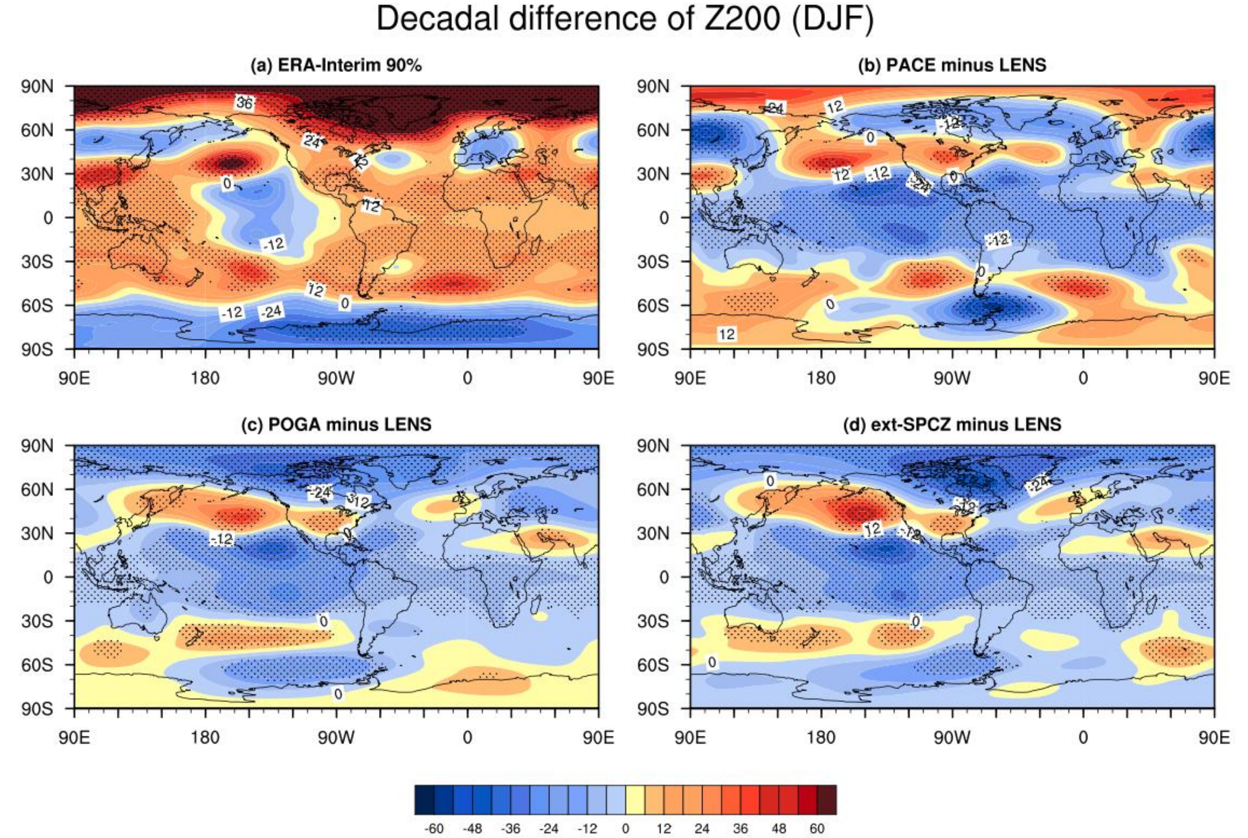

Figure 3. Decadal difference (P2-P1) of 200 hPa geopotential height for (a) ERA-Interim; (b) PAC-EM minus LENS; (c) POGA minus LENS; (d) ext-SPCZ minus LENS. Stippling indicates differences are significant at the 95% level based on a t-test.